

Article

Effects of a Bulbous Bow Shape on Added Resistance Acting on the Hull of a Ship in Regular Head Wave

Trung-Kien Le ^{1,*}, Ngo Van He ^{2,*}, Ngo Van Hien ^{2,*} and Ngoc-Tam Bui ^{1,3,*}

- ¹ School of Mechanical Engineering (SME), Hanoi University of Science and Technology (HUST), No.1 Dai Co Viet, Hanoi 10000, Vietnam
 - ² School of Transportation Engineering (STE), Hanoi University of Science and Technology (HUST), No.1 Dai Co Viet, Hanoi 10000, Vietnam
 - ³ College of Systems Engineering and Science (CSES), Shibaura Institute of Technology (SIT), Tokyo 135-8548, Japan
- * Correspondence: kien.letrung@hust.edu.vn (T.-K.L.); he.ngovan@hust.edu.vn (N.V.H.); hien.ngovan@hust.edu.vn (N.V.H.); tambn@shibaura-it.ac.jp (N.-T.B.)

Abstract: In this study, the effect of bow shape on resistance acting on a hull in regular head waves was investigated by applying a commercial Computational Fluid Dynamics (CFD) code. For this purpose, the hydrodynamic performance as well as the resistance of ships with blunt and bulbous bows were simulated. By analyzing the obtained CFD simulation results, the effects of the bow shape on the hydrodynamic performance and resistance of the ships were found. A new bulbous bow shape with drastically reduced added resistance acting on the hull in waves is proposed. Finally, the obtained CFD results for the hydrodynamic performance of ships are presented.

Keywords: resistance; CFD; regular head waves; hull; bulbous bow; hydrodynamic



Citation: Le, T.-K.; He, N.V.; Hien, N.V.; Bui, N.-T. Effects of a Bulbous Bow Shape on Added Resistance Acting on the Hull of a Ship in Regular Head Wave. *J. Mar. Sci. Eng.* **2021**, *9*, 559. <https://doi.org/10.3390/jmse9060559>

Academic Editor: Nikos Themelis

Received: 18 April 2021
Accepted: 20 May 2021
Published: 21 May 2021

Publisher's Note: MDPI stays neutral with regard to jurisdictional claims in published maps and institutional affiliations.



Copyright: © 2021 by the authors. Licensee MDPI, Basel, Switzerland. This article is an open access article distributed under the terms and conditions of the Creative Commons Attribution (CC BY) license (<https://creativecommons.org/licenses/by/4.0/>).

1. Introduction

A bulbous bow is a long-established solution for reducing the added resistance acting on ships by using the bulbous bow's wave-generating effect. The study of reducing added waves' resistance as well as reducing the total resistance of ships so as to reduce fuel consumption is still an important topic in the marine transportation field. For ships with huge hulls and blunt bows, the resistance from added waves acting on the hull accounts for a large percentage of the total resistance in conditions of both calm water and waves. Therefore, many researchers around the world have given importance to the study of reducing added waves' resistance acting on ships' hulls.

In recent years, a large number of published papers have examined the topics of reduced added waves' resistance on ships, optimal hydrodynamic hull shapes, the effects of bow and stern shapes on added waves' resistance, and the optimal hull shape in wave conditions, etc. We offer a comprehensive literature review below.

There are many published papers on applying a commercial Computational Fluid Dynamics (CFD) code to investigate ship hydrodynamic performance. CFD has been a useful and popular tool for solving problems of the hydrodynamic performance of ships with high accuracy. By applying CFD, various hull forms with small resistances have been proposed [1–16].

The Non Ballast Water Ship (NBS) model has been known since 2010, when it was developed at the laboratory of Prof. Ikeda at Osaka Prefecture University (OPU). Tatsumi et al. (2010) presented a study on the development of a new energy-saving NBS tanker with multiple podded propulsors. The ship was developed with a round and streamlined hull to drastically reduce viscous resistance and multiple podded propulsors moving up and down to keep the propellers deep enough in the water. Using an experimental model in the towing tank at OPU for several hull forms, their results confirmed that the resistance

acting on the new ship was reduced by up to 44.8% of the total resistance with ballast, and up to 17.5% at full load [17]. The original hull form with a blunt bow shape was proposed at first. The experimental model test demonstrated that, at a low Froude number of less than 0.16, the resistance acting on the original ship was significantly higher because of the possibly increase in wave resistance [18,19].

Tomita et al. (2011) and Tasumi et al. (2011) presented a study on developing a new bulbous bow for the original NBS model with reduced added resistance at the hull, achieved using an experimental model in a towing tank. The ships with the new bow shape could reduce the total resistance in calm water by up to 11%. Additionally, the model could reduce the added waves' resistance in moderated short waves by up to 25%; the waves' height (H_w) was 0.02 m and the waves' length per ship length (λ/L_{pp}) was less than 0.6 for the 2 m long model tested in the towing tank [18,19]. In other research on the development of a new bow form for the NBS performed at Ikeda's laboratory at the OPU, a commercial CFD code was applied to optimize the bow shape. The ship resistance, both in calm water and in wave conditions, was the object of the optimization process for designed parameters such as the volume of the bow shape, the height of the volume at the center of the bow, the angle of the bow's bottom, and the length of the bow. Analysis of the results showed that the optimal bulbous bow shape could reduce the total resistance of the hull form by up to 15% in calm water and by up to 18% in regular head wave conditions ($H_w = 0.02$ m; $\lambda/L_{pp} < 0.6$) [2–4,20–22].

Luo et al. (2016) presented a study on the optimal design of the lines of a bulbous bow shape using applied parametric modeling and CFD computation. In the study, the lines of the ship's bow were optimized by using an optimal platform at the hull shape design stage using automatic progress. Additionally, the Rankine source panel method was applied to evaluate the added waves' resistance acting on the hull of a Ro-Ro ship. The results showed that added wave resistance was clearly reduced and the wave bow profile became gentle in the ship design with optimized lines of the bulbous bow [23]. Others studies also used the Rankine source panel method; for example, Lu et al. (2016) presented a study of an innovative method for the optimization of the hydrodynamic performance of a bulbous bow while considering different conditions [24]. Zhang et al. (2017) presented research on the optimal bulbous bow shape based on the newly improved PSO algorithm. In the study, the total resistance of the ship in calm water was defined as the objective function, and the overset generated mesh method was applied to meshing. The volume of fluid method, together with the Reynolds Averaged Navier–Stokes (RANS) equation, was applied to evaluate the resistance acting on the hull [25].

Lee et al. (2019) presented research on the effects of bow form on ship resistance in both calm water and wave conditions for the 66,000 DWT bulker carrier. In the study, a computational tool was used to clearly find the cause of reduced resistance acting on the ship hull in both calm water and wave conditions for the sharp bow shape in comparison to the blunt bow shape of the 66,000 DWT bulker carriers. The unsteady flow with two phases method, the RANS equations, and the turbulent viscous $k-\epsilon$ model were applied to a realizable model. The results showed good agreement between the CFD and experimental towing tank results. The pressure viscous resistance of the ship in calm water and wave conditions with the sharp bow shape could be reduced by up to 8.9% and 12.7%, respectively, in formed head waves compared with those of the hull with a blunt bow shape [26].

Other published papers reported on the hydrodynamics and resistant hull forms of different hulls of ships studied using experimental measurements at towing tanks and CFD computation. Begovic et al. (2014) presented a result of a model towing tank test on sea-keeping assessment of a ship with a warped planning hull series [27]. Casalone et al. (2020) presented a study on unsteady RANS computational fluid dynamic simulations of sailboats and compared their results with the resistance results of the full scale experiment [12]. Feng et al. (2020) presented a study on the numerical computation of resistance acting on the hull of a KCS ship at different depth conditions for a scale computed model and the full

scale model [13]. Ngo (2017) presented a study on a newly developed reduced concept for river ships in calm water [28]. Kahramanoğlu et al. (2020) presented a study on a numerical simulation used to predict the component vertical responses of planning ships under wave conditions [14]. Sun et al. (2020) studied numerical computation used to investigate ship resistance and ship motion stability for a high-speed planning trimaran [15]. Other similar studies include [11,16,29].

In this study, a commercial CFD tools named ANSYS-Fluent v.15.0 has been applied to investigate the effect of a bulbous bow shape on ship resistance, both in calm water and in regular head waves conditions. The original hull form of the NBS with a blunt bow form, which was developed by Prof. Ikeda at Osaka Prefecture University, was used as a reference ship model. By using the CFD, the hydrodynamic performance and resistance acting on the hulls with and without a bulbous bow shape were simulated to determine the effect of the bulbous bow shape. From the obtained results, a new hull shape with a bulbous bow and reduced added resistance has been clearly identified in this study.

2. The Reference Model and Simulating Domain

2.1. The Reference Model Used for Simulation

In this research, the original hull form of the NBS was used as a reference model to validate the CFD results and investigate the effect of bow shape on the added waves' resistance of the ship. The original NBS was developed at the laboratory of Professor Ikeda of OPU in 2010. The ship was designed with a blunt bow shape and round cross section to reduce viscous resistance in calm water [2,3,17,19–21]. The principal dimensions of the original NBS are shown in Table 1. The designed original NBS hull shape is shown in Figure 1.

Table 1. Principal dimensions of the original NBS.

No.	Description	Value	Unit
1	Length of the ship, L_{pp}	2.000	m
2	Depth of the ship, H	0.181	m
3	Breadth of the ship, B	0.359	m
4	Draft of the ship, d	0.131	m
5	Displacement of the ship, D	0.06504	ton
6	Wetted surface area, S	0.921	m ²
7	Block coefficient, C_b	0.691	-

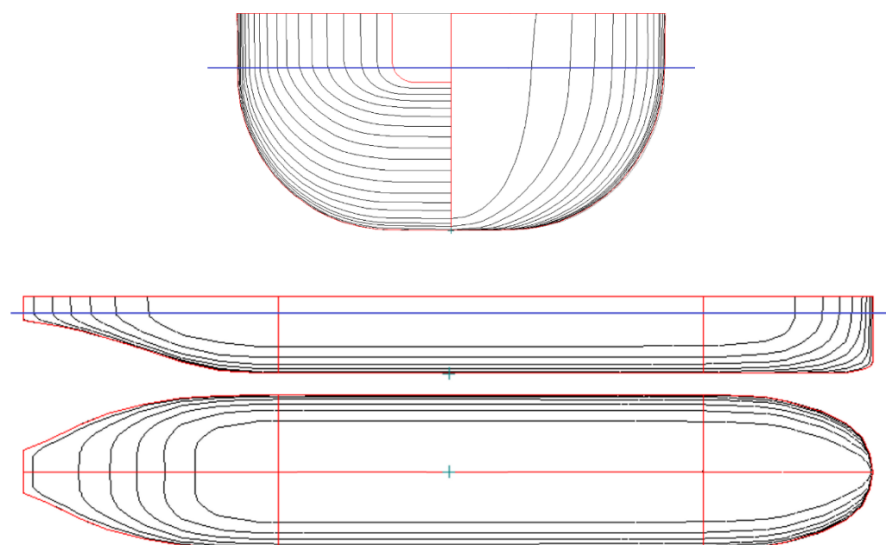


Figure 1. Original NBS developed by Professor Ikeda of OPU in Japan [2,3,17].

2.2. Simulating Domain and Setup Boundary Conditions

In the CFD computation, the steps of the simulation include designing the computation domain, generating a mesh, and setting up the computed conditions, all of which must be conducted as per the user guideline documents, which have been published as the International Towing Tank Conference (ITTC) manual for applying the CFD code [30–35] and previous publications [2–4,8,9,20,21,28,30,32,35–39]. In this study, the computed fluid domain has been limited to 6.5, 0.55, and 0.75 L instead of 13 m length, 1.1 m breadth, and 1.5 m height. Meshing the simulated domain in the structured H-grid was generated in 2.63 million grids. The turbulent viscous model $k-\omega$, applied to unsteady flow and the Volume of Fluid (VOF) multiphase model, were used. The inlet and outlet of the computed domain were set up with a velocity inlet and a pressure outlet. In the CFD simulation, the simulated domain should be designed to be large enough for the problem. However, the limited dimensions of the simulated domain affect the size of the mesh, as well as affecting the hardware and the running time. The effects of the limited dimensions of the computed domain on the CFD results will become small if the computed domain is large enough. Therefore, we must design an optimal computed domain and set up appropriate boundary conditions. In this study, the time step was set up to be 0.005 s, and the running time included 6000 time steps. Figure 2 shows the simulated domain and the generated mesh in the H-grid structure used for the computation.

In the CFD computation, the effects of the mesh of the computed domain on the CFD results have been reported in many previous papers [2,3,13–15,30,35,39]. Moreover, in the computation of ship resistance in waves, the height and size of the mesh at the free surface of the computed domain determine the accuracy of the incident wave profile. Therefore, we must make an appropriated mesh for the computed domain. In this study, we independently generated results regarding the resistance acting on the hull of the mesh in the computational domain in CFD. Conditions of both calm water and waves have been simulated in different scenarios; at the Froude number of 0.163, the wave height is 0.02 m and wave length is 0.8 m. Table 2 lists details of the mesh of the computed domain and the computed ship resistance coefficients in the different computed cases. Figure 3 shows the curves of the mesh effect on the computed ship resistance coefficients in calm water and in regular head waves.

Figure 3 shows the results of the different resistance coefficients (ΔC_T) in the different computed cases listed in Table 2. The results show that the differences among the computed resistance coefficients in calm water were smaller than those of the ship in wave conditions. The difference between the computed results was less than 10% when the value of $y+$ was less than 1.057, as shown. In calm water, when the mesh number was over 1.488 million instead of a $y+$ value below 1.592, the resistance coefficient was the same for all computed cases. In regular wave conditions, the different resistance coefficients were close when the $y+$ value was below 0.872, as shown.

Table 2. Details of the mesh and the CFD results of ship resistance coefficients.

No.	$y+$	Total Elements ($\times 10^6$)	Minimum Face Area, m^2 ($\times 10^{-8}$)	Maximum Face Area, m^2 ($\times 10^{-4}$)	Minimum Volume, m^3 ($\times 10^{-6}$)	Maximum Volume, m^3 ($\times 10^{-2}$)	$C_{T(0)}$ ($\times 10^{-2}$)	$C_{T(W)}$ ($\times 10^{-2}$)
1	7.221	0.783	1.5226	12.2256	2.6854	3.2564	0.4921	0.5679
2	5.772	0.868	1.2256	9.6255	2.3566	2.9265	0.5010	0.5810
3	3.616	1.057	1.0500	8.0123	2.0952	2.7326	0.5124	0.6133
4	1.592	1.488	0.2840	2.9620	1.1325	0.9958	0.5176	0.6325
5	1.328	1.822	0.0126	2.8423	0.0562	0.9965	0.5181	0.6384
6	0.872	2.368	0.1193	2.2821	0.3752	1.0921	0.5189	0.6429
7	0.582	3.286	0.0295	2.0123	0.1265	1.2446	0.5201	0.6468
8	0.363	5.682	0.0156	1.9852	0.0625	1.1955	0.5198	0.6479
9	0.221	7.524	0.0184	2.9621	0.0326	0.6955	0.5204	0.6489

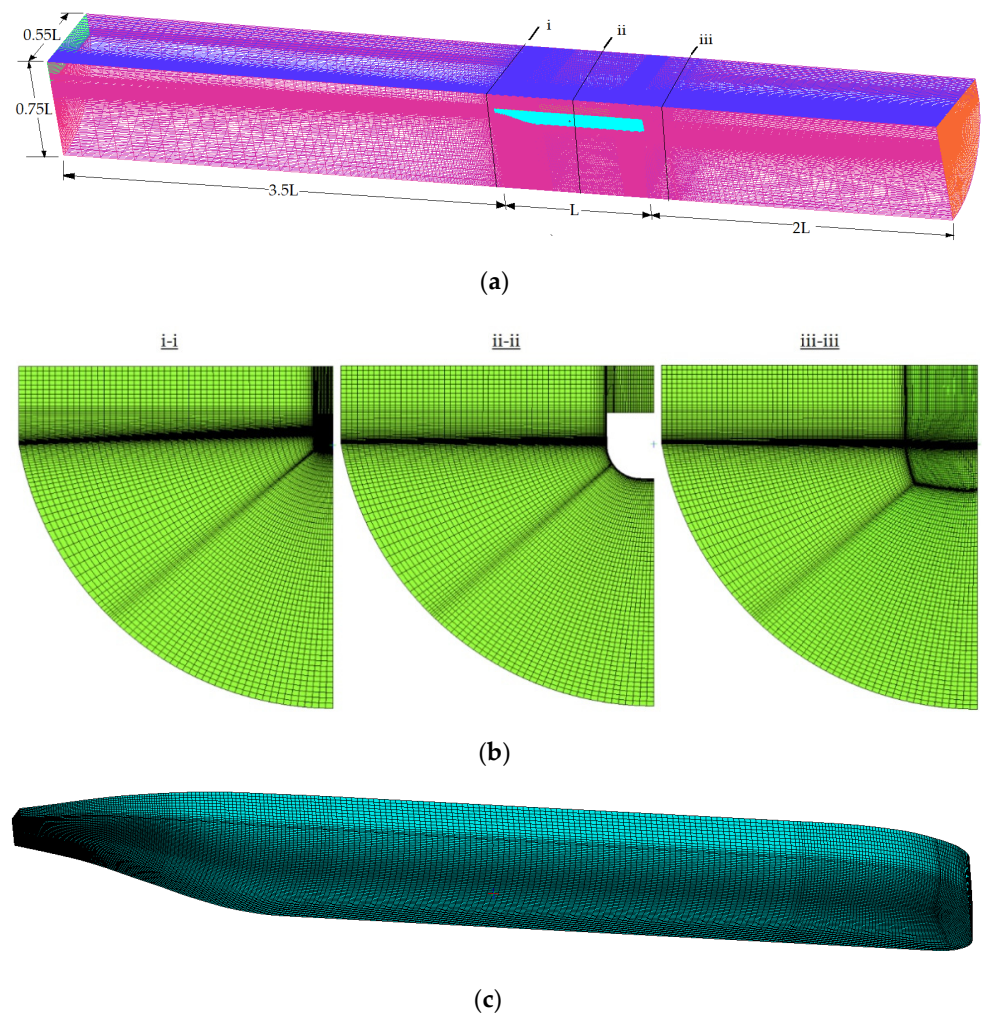


Figure 2. Simulated domain and structured mesh. (a) Mesh of simulated domain; (b) mesh at several cross sections in the simulated domain; (c) mesh in the hull surface of the model.

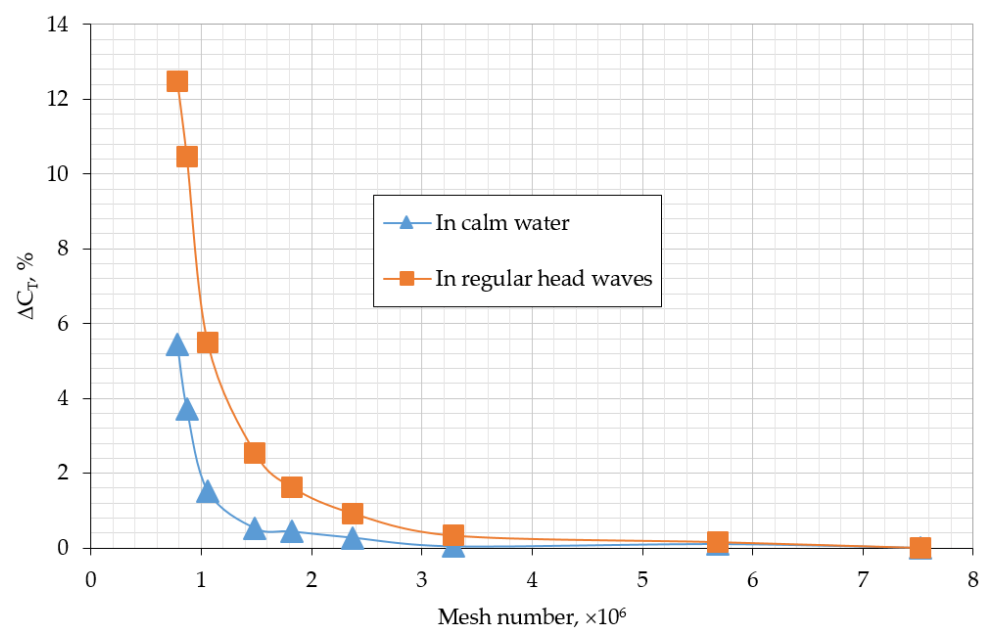


Figure 3. Effect of mesh number on CFD results of total resistance coefficient of the ship in calm water and in regular head waves at $F_n = 0.163$, $H_w = 0.02$ m, and $\lambda/L_{pp} = 0.4$.

2.3. Validation of the Used CFD

In this research, we performed a comparison between the CFD results and the obtained experimental data of the model test at the towing tank at OPU. The original NBS model with a length of 2 m was used for computation, and the experiment investigated the hydrodynamic performance as well as the hull resistance, both in calm water conditions and in regular head waves. Figures 4 and 5 show the results of the comparison regarding the resistance acting on the model in the CFD simulation and the experiment at the towing tank [2,3,17–19].

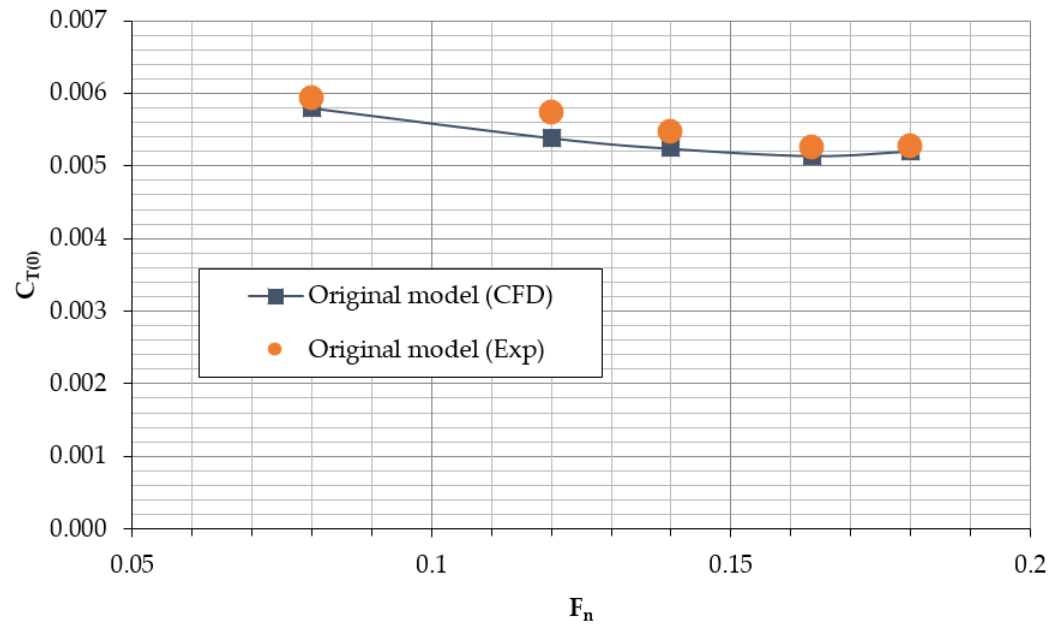


Figure 4. Comparison between the CFD results and experimental data of resistance acting on the ship in calm water.

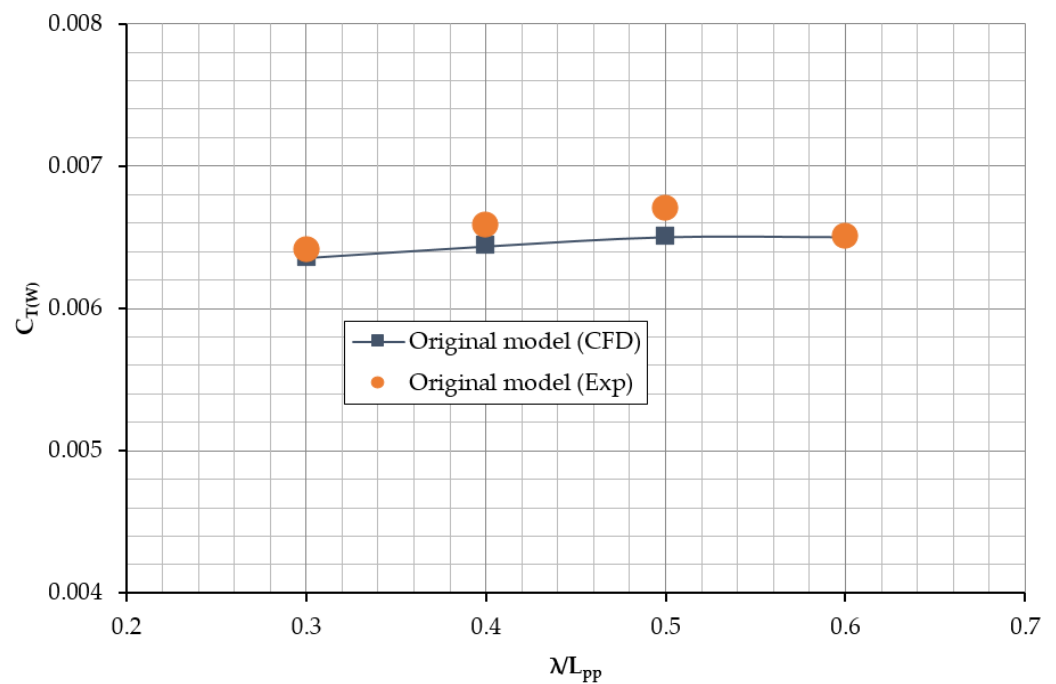


Figure 5. Validation of CFD results of the total resistance coefficients of the ship in regular head and short waves, $H_w = 0.02$ m, $F_n = 0.163$.

Figures 4 and 5 show a comparison between the CFD results of the total ship resistance coefficients and the experimental data, both in calm water conditions and in regular head and short waves. The total ship resistance coefficients in calm water, $C_{T(0)}$, and the total ship resistance coefficients in regular head and short waves, $C_{T(W)}$, are defined by the following equation:

$$C_T = \frac{R_T}{0.5\rho SV^2} \tag{1}$$

where:

C_T is the total resistance coefficient;

R_T is the total resistance acting on the hull, N;

S is the wetted surface area, m^2 ;

ρ is the water density, kg/m^3 ;

V is the velocity of the ship, m/s .

The results presented in Figures 4 and 5 show a comparison between the total ship resistance coefficients computed by the CFD and experimental data of the towing tank model test. The agreement between the computed results and the experimental results is fairly good, as shown. In calm water conditions, the difference between the CFD results and the experimental results is less than 6% in the range of the Froude number from 0.08 to 0.18, as shown in Figure 4. Figure 5 shows a good agreement between the CFD results and the experimental data of the total ship resistance in waves, where the incident waves are short and regular head waves, the λ/L_{pp} is less than 0.6, and the wave height, H_w , is 0.02 m for the 2 m length of the model at the Froude number of 0.163. The obtained results demonstrate the usefulness of applying CFD to compute the resistance and hydrodynamic performance of ships.

3. Effect of Bulbous Bow on the Hydrodynamic Performance of the Ship

3.1. Model of the NBS with the Newly Proposed Bow Shape

In this study, a new bow shape was proposed for the NBS to reduce the added resistance of the hull form. The original ship has a blunt bow shape, whereas the new hull has a developed bow shape; the two ships have the same principal dimensions and stern shapes and only differ in their bow shapes. By using the CFD, the ships were computed and the obtained CFD results were compared so as to find out the effects of bow shape on the ships' hydrodynamic performance.

Figure 6 shows the models of a new hull with a bulbous bow shape used for the computation; detailed principal dimensions of the model are listed in Table 3.

Table 3. Principal dimensions of the bulbous bow model.

No.	Description	Value	Unit
1	Length of the ship, L_{pp}	2.120	m
2	Depth of the ship, H	0.181	m
3	Breadth of the ship, B	0.359	m
4	Draft of the ship, d	0.131	m
5	Displacement of the ship, D	0.0661	ton
6	Wetted surface area, S	0.965	m^2
7	Block coefficient, C_b	0.678	-

3.2. Effect of Bow Shape on Pressure Distribution of the Ships in Calm Water

In this section, the CFD results of the pressure distributions around the ships in calm water are shown. Figures 7 and 8 show comparison of pressure distribution around the hull at the free surface of the computed domain of the ships, at the Froude number of 0.163 in calm water conditions.

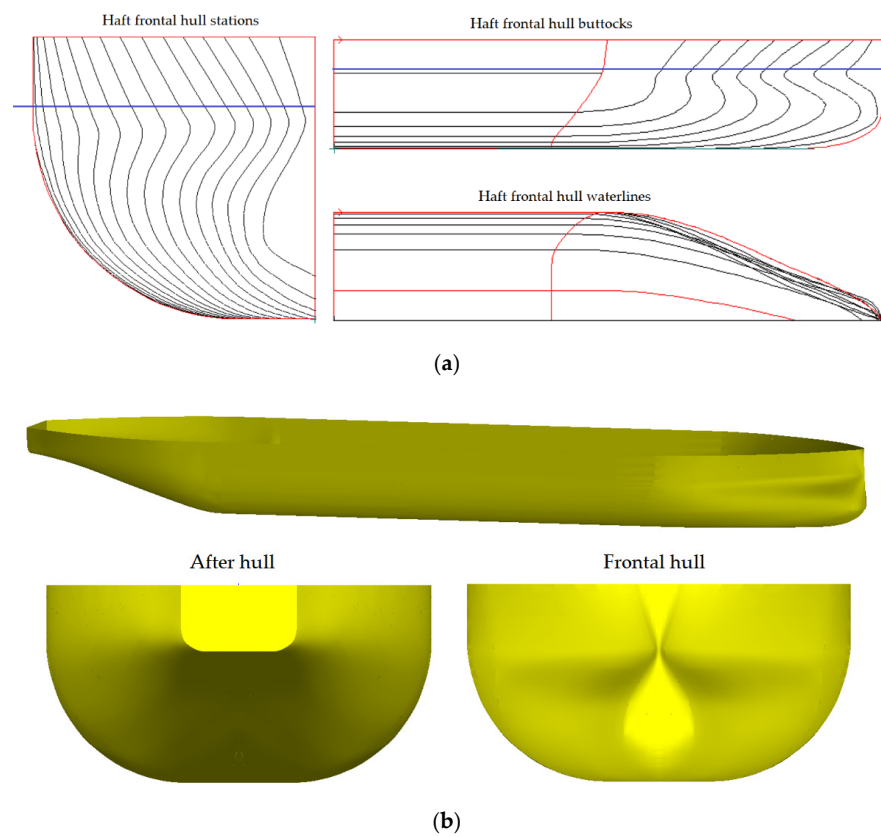


Figure 6. Models of NBS with a bulbous bow used for simulation. (a) Haft frontal body plan of the new bulbous bow model; (b) new proposed model used for CFD computation.

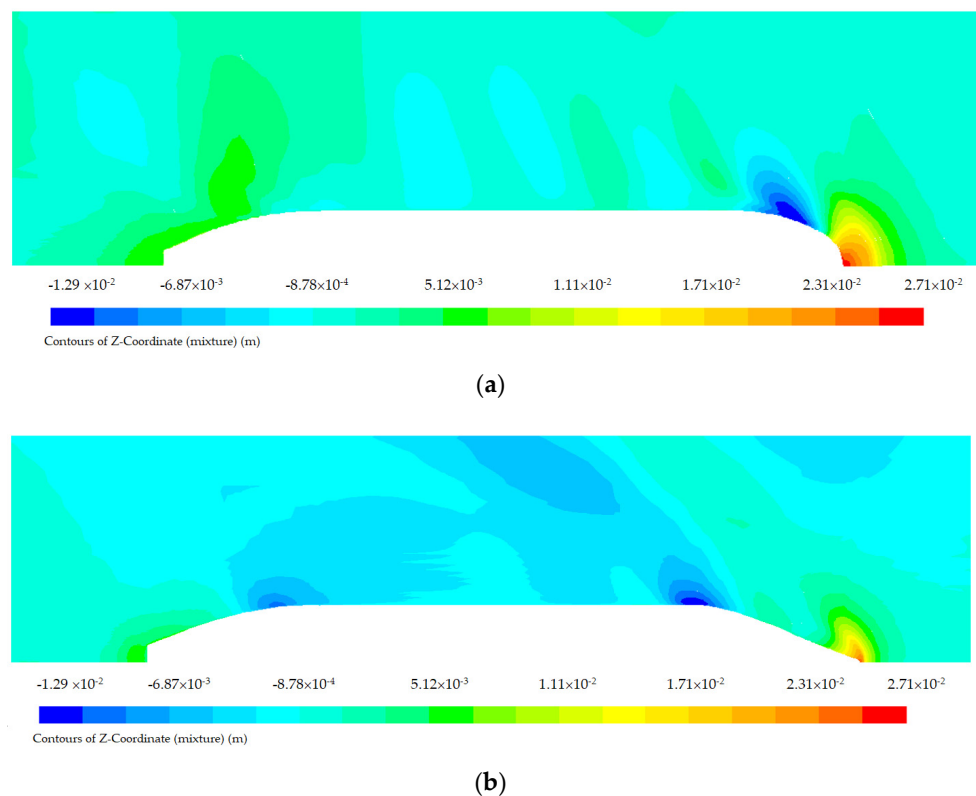


Figure 7. Simulated wave pattern at the free surface of the ships at $F_n = 0.163$ in calm water conditions. (a) The NBS with a blunt bow shape; (b) the new hull with a newly developed bow shape.

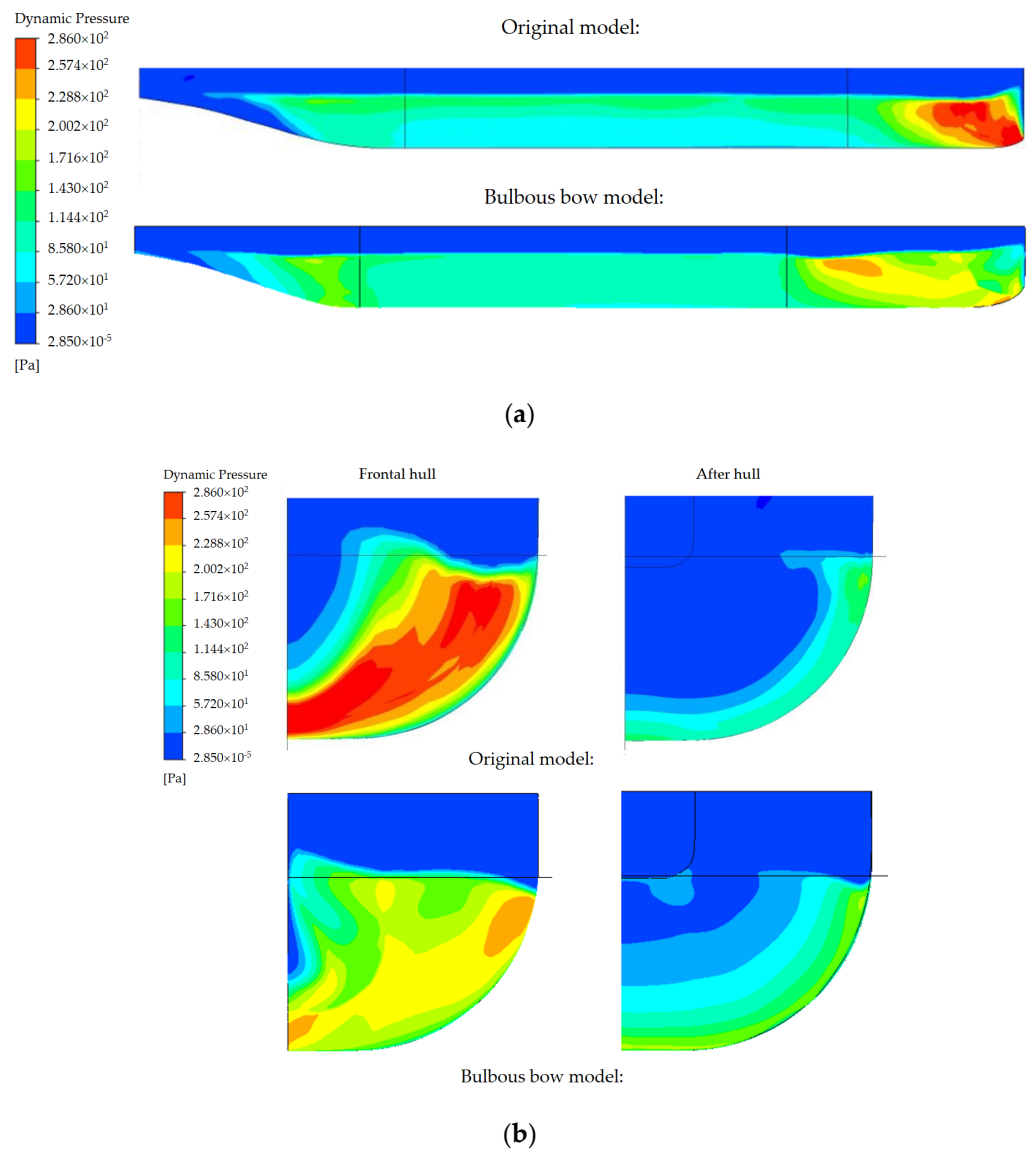


Figure 8. CFD results of dynamic pressure distribution over the surface of the ship’s hulls at $F_n = 0.163$ in calm water conditions. (a) Side view; (b) frontal and aft view.

In Figure 7, the red and yellow regions indicate that the generated waves are high, and the blue region indicates deep waves made by the ship running in calm water conditions. The results clearly show waves of reduced height and depth in the region around the frontal hull of the ship with the developed bulbous bow shape. Figure 8 shows the dynamic pressure distribution over the surface of the hull at the Froude number of 0.163 in calm water conditions.

Analyzing the dynamic pressure distribution, as shown in Figure 8, the red and yellow regions indicate high dynamic pressure and the blue region indicates a lower dynamic pressure region over the surface of the ship’s hulls. The results show drastically reduced high dynamic pressure regions over the surface of the ship’s hull with a bulbous bow shape. The effects of the bow shape on the pressure distribution over the surface of the ship’s hull could be evaluated. The effects of the bulbous bow shape on the pressure distribution of the ships may be evaluated by a comparison between the ship resistance in the two cases of the computation with and without a bulbous bow shape.

3.3. Effect of Bulbous Bow Shape on Ship Pressure under Regular Head Waves Conditions

In this study, the NBS ship with and without a bulbous bow shape was simulated under wave conditions. The incidence of waves at the regular head and the short waves with $H_w = 0.02$ m and a ratio of λ/L_{pp} was less than 0.6. Figure 9 shows the CFD results of wave patterns at the free surface of the simulated domain under wave conditions at $\lambda/L_{pp} = 0.4$, with the Froude number of 0.163.

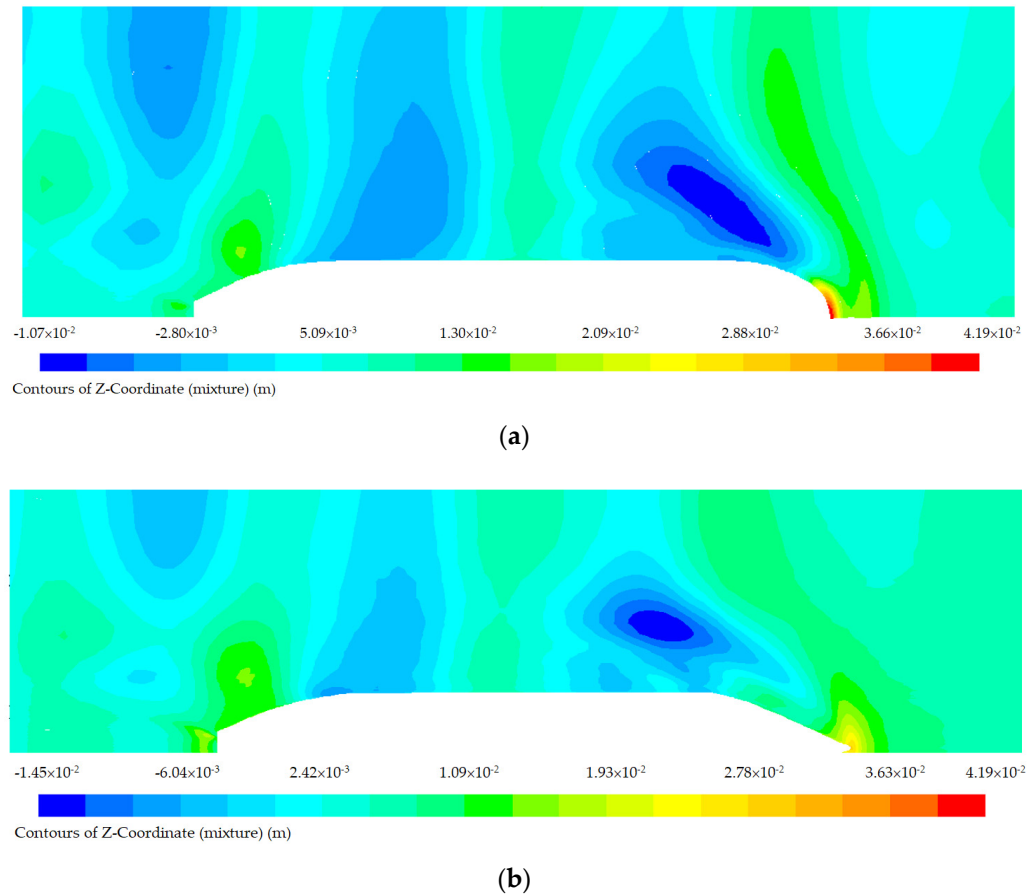


Figure 9. Simulated wave patterns at the free surface of the ships at $F_n = 0.163$ with regular head waves. (a) The original model; (b) the new model with a bulbous bow.

The results, as seen in Figure 9, show a wave pattern at the free surface of the simulated domain when the ships run under wave conditions with a wave height of 0.02 m and the ratio $\lambda/L_{pp} = 0.4$ for the 2 m long model, at the Froude number of 0.163. In the results, the high and deep waves around the ships’ bows are different with and without the developed bulbous bow. Figure 10 shows a comparison of the dynamic pressure distribution over the surface of the ship’s hulls under wave conditions.

Analyzing the CFD results of dynamic pressure, as shown in the Figure 10, the bow wave made by the original hull without the bulbous bow is clearly higher than that of the bulbous bow model. The high dynamic pressure area region (red and yellow regions) and low dynamic pressure area regions (blue regions) acting over the hull surface of the bulbous bow model are drastically reduced. The results demonstrate that the new bulbous bow shape may reduce ship resistance under wave conditions.

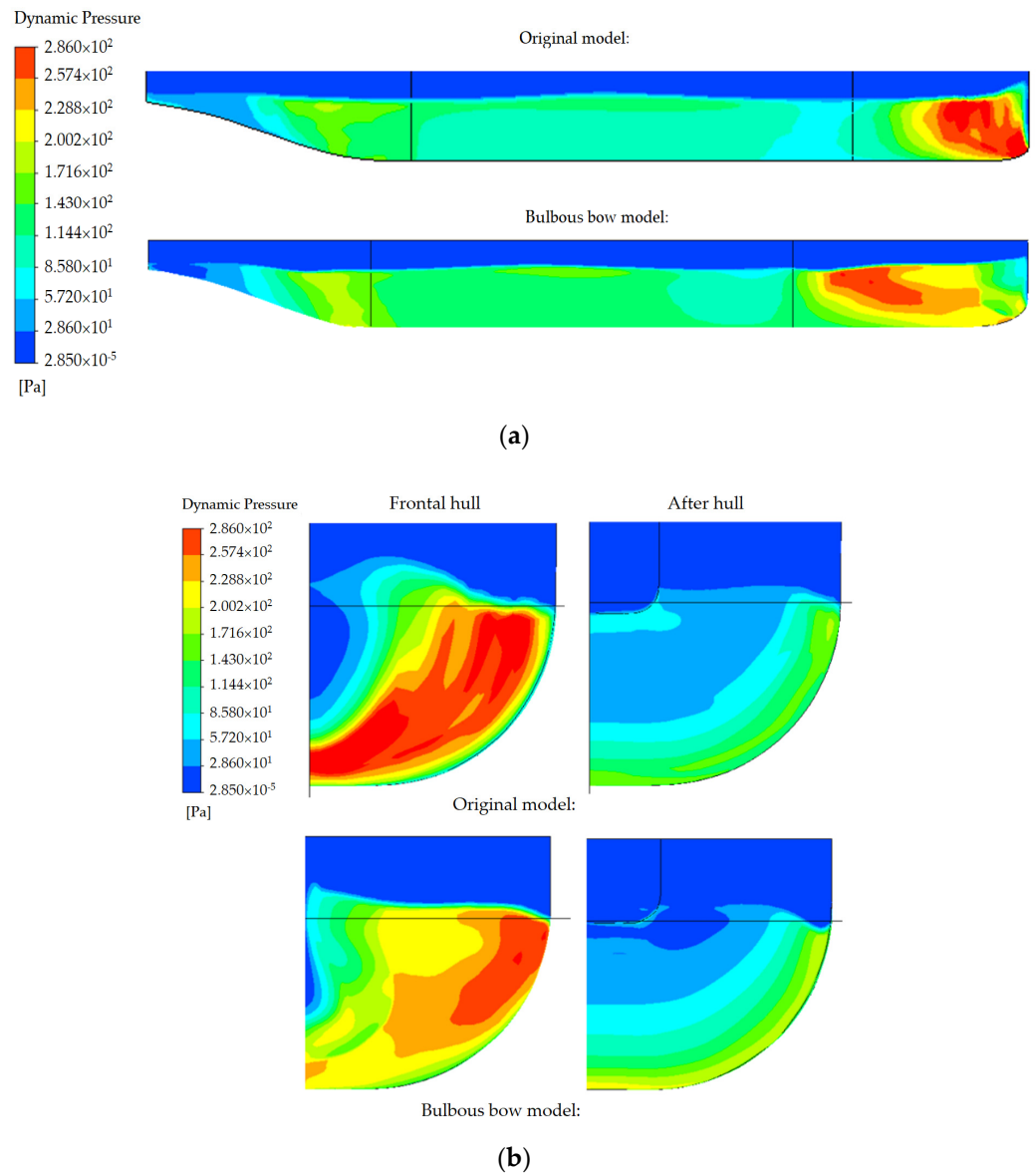


Figure 10. Simulated dynamic pressure distribution over the surface of the ship’s hulls in regular head and short waves, $H_w = 0.02$ m and the ratio $\lambda/L_{pp} = 0.4$, at $F_n = 0.163$. (a) Side view; (b) frontal and aft view.

4. Reduced Ship Resistance

4.1. Ship Resistance in Calm Water

In this study, resistance acting on the hulls of the NBS in calm water was computed by the CFD. By comparison of the ship resistance between the two ships, one with a blunt bow and one with a bulbous bow shape, the effect of the bow shape on the resistance of the NBS in calm water conditions has been found. The detailed computed results of ship resistance for the 2 m-long models in calm water conditions are listed in Tables 4 and 5. Figure 11 shows a comparison of the total resistance coefficients of the two ships in calm water conditions.

Table 4. Resistance acting on the original model in calm water.

Resistance (N)				Resistance Coefficients		
F_n	R_p	R_f	R_T	C_p	C_f	C_T
0.080	0.0324	0.3020	0.3343	0.00056	0.00523	0.00579
0.120	0.1122	0.5869	0.6991	0.00086	0.00452	0.00538
0.140	0.1742	0.7535	0.9276	0.00098	0.00426	0.00524
0.163	0.2705	0.9706	1.2411	0.00112	0.00402	0.00514
0.180	0.3699	1.1526	1.5225	0.00126	0.00394	0.00521

Table 5. Resistance acting on the bulbous bow model in calm water.

Resistance (N)				Resistance Coefficients		
F_n	R_p	R_f	R_T	C_p	C_f	C_T
0.080	0.0169	0.3189	0.3357	0.00028	0.00532	0.00560
0.120	0.0430	0.6422	0.6852	0.00032	0.00476	0.00508
0.140	0.0672	0.8388	0.9060	0.00037	0.00456	0.00493
0.163	0.0996	1.1268	1.2264	0.00040	0.00450	0.00489
0.180	0.1304	1.3618	1.4922	0.00043	0.00448	0.00491

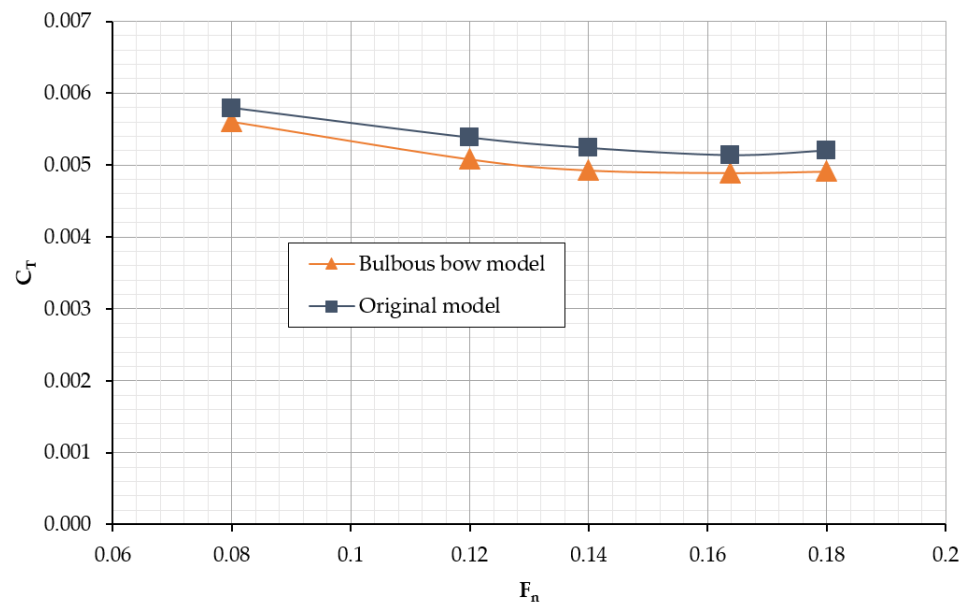


Figure 11. Comparison of the total resistance coefficients of the ships.

In the computation, ship resistance was divided into the two components of pressure viscous resistance (R_p) and frictional viscous resistance (R_f), the total resistance (R_T) is defined following Equation (1), and the total resistance coefficient is defined as follows:

$$C_T = C_p + C_f \tag{2}$$

where:

C_p is the pressure viscous resistance;

C_f is the frictional viscous resistance coefficient.

The results of the total resistance coefficients of the ships shown in Tables 4 and 5 and Figure 11 show that the frictional viscous resistance acting on the bulbous bow model was slightly higher than that of the original model, which may be the result of the larger wetted surface area of the bulbous bow shape. Additionally, the pressure viscous resistance and the total resistance acting on the bulbous bow model were smaller than those of the

original model by up to 6%. The reasons for this may arise from the effects of the developed bulbous bow shape.

4.2. Ship Resistance under Wave Conditions

In this study, the effect of the bow shape on ship resistance under conditions of regular head waves was investigated via comparison with the other CFD results of the two ships with and without the bulbous bow. Tables 6 and 7 list the detailed ship resistance under wave conditions with $H_w = 0.02$ m for the 2 m-long model, at the Froude number of 0.163. Figures 12 and 13 show a comparison of the computed ship resistance under wave conditions for the two ships.

Table 6. Computed ship resistance of the original model under wave conditions.

λ/L_{pp}	Resistance (N)			Resistance Coefficients		
	R_P	R_F	R_T	C_P	C_F	C_T
0.3	0.8151	0.9069	1.7220	0.00253	0.00383	0.00636
0.4	0.7116	0.9523	1.6638	0.00248	0.00395	0.00644
0.5	0.7344	0.9591	1.6935	0.00257	0.00393	0.00650
0.6	0.7706	0.9541	1.7248	0.00262	0.00388	0.00650

Table 7. Resistance acting on the bulbous bow model in waves.

λ/L_{pp}	Resistance (N)			Resistance Coefficients		
	R_P	R_F	R_T	C_P	C_F	C_T
0.3	0.3381	1.0466	1.3847	0.00135	0.00418	0.00552
0.4	0.3725	1.0291	1.4016	0.00149	0.00411	0.00559
0.5	0.3769	1.0386	1.4155	0.00150	0.00414	0.00565
0.6	0.3699	1.0484	1.4183	0.00148	0.00418	0.00566

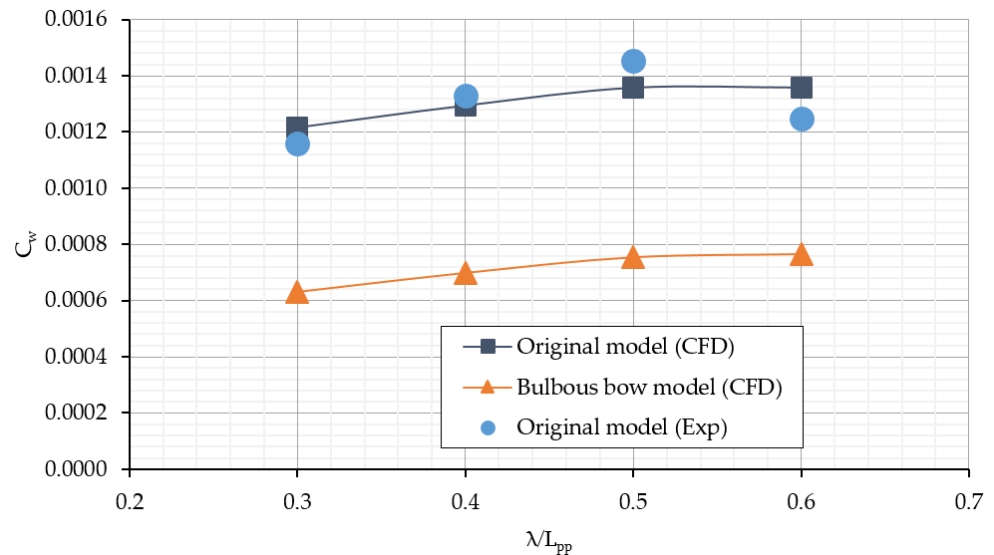


Figure 12. Added wave resistance coefficients of the ships under wave conditions, $H_w = 0.02$ m at $F_n = 0.163$.

In the research, the added wave resistance under wave conditions is defined as in the following equation:

$$C_W = C_{T(W)} - C_{T(0)} \tag{3}$$

where:

$C_{T(0)}$ is the total ship resistance coefficient in calm water conditions;

$C_{T(W)}$ is the total ship resistance coefficient under wave conditions.

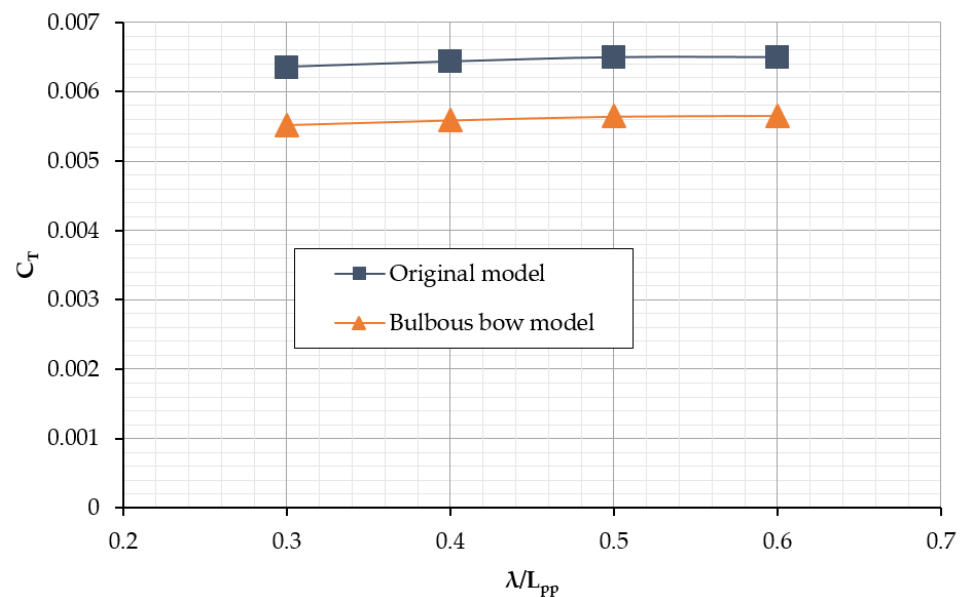


Figure 13. Total ship resistance coefficients under the condition of regular head waves, $H_w = 0.02$ m at $F_n = 0.163$.

The results of ship resistances detailed in Tables 6 and 7 clearly show the ship resistance of the two ships under the condition of regular head waves for the 2 m-long model, at $H_w = 0.02$ m and $F_n = 0.163$. The results in Figures 12 and 13 clearly show the effects of the new bow shape on the resistance acting on the ship under wave conditions. The added wave resistance coefficients of the new bow model have been drastically reduced by up to 48% compared with those of the blunt bow model, as shown. Additionally, the total ship resistance of the ship with the developed bulbous bow was reduced by up to 13%. The results of ship resistance were also in good agreement with the obtained CFD results of the pressure distribution and the experimental data, as shown. The proposed bulbous bow shape could thus be a good choice for the NBS to reduce resistance.

However, to clearly find the full effects of the bulbous bow shape on the resistance acting on the ship, we need more comparable results regarding the ships running under different conditions, including ballast conditions and in different wave conditions at other Froude numbers. In this study, we only aimed to show an appropriate bulbous bow shape at the designed draft condition and designed speed under the full load condition of the ships running in calm water and in regular head waves. The incident wave considered was a regular head wave with a wave height $H_w = 0.02$ m and ratio of $\lambda/L_{pp} < 0.6$ at the designed speed of $F_n = 0.163$; we will examine other conditions in our future work.

5. Conclusions

In this study, the hydrodynamic performance and the resistance of the NBS with and without a bulbous bow shape under full load conditions were investigated using the CFD. From the obtained results, the effect of bow shape on ship resistance has been shown. Furthermore, the CFD results obtained in this study show that the new hull form with a proposed bulbous bow shape can be applied to considerably reduce the added wave resistance as well as to reduce fuel consumption. The main conclusions of this study are summarized as follows:

- The obtained CFD results for the two ships, namely, the original NBS hull with a blunt bow shape and one with a new bulbous bow shape in the full load condition, were obtained. It was confirmed that the CFD code provided us with good results regarding

the computed resistance acting on the hull of the ship, both under calm water and in regular head wave conditions.

- The proposed bulbous bow shape had effects on the hydrodynamic performance as well as the ship resistance of the NBS in the computed condition. It has been clearly shown that the developed bulbous bow shape affected both the pressure distribution and the wave pattern at the free surface of the ship in the computed domain. Hence, an appropriate bulbous bow shape could be developed to drastically reduce the total resistance in the computed condition.
- The effects of the bulbous bow shape on reduced resistance acting on the NBS in calm water reached about 6% in the case of the higher wetted surface area of the bulbous bow model.
- The effect of a bulbous bow shape on the resistance acting on the hull under regular head wave conditions with $H_w = 0.02$ m and the ratio $\lambda/L_{pp} < 0.6$ was investigated. Using the proposed bulbous bow shape, up to 48% of the added wave resistance and 13% of the total resistance acting on the hull of the NBS at the Froude number of 0.163 in the computed wave condition could be reduced.

Author Contributions: Conceptualization, T.-K.L., N.V.H. (Ngo Van He), N.V.H. (Ngo Van Hien) and N.-T.B.; methodology, T.-K.L., N.V.H. (Ngo Van He), N.V.H. (Ngo Van Hien) and N.-T.B.; software, N.V.H. (Ngo Van He) and N.V.H. (Ngo Van Hien); validation, N.V.H. (Ngo Van He), N.V.H. (Ngo Van Hien) and N.-T.B.; writing—original draft preparation, T.-K.L. and N.V.H. (Ngo Van He), N.V.H. (Ngo Van Hien); writing—review and editing T.-K.L., N.V.H. (Ngo Van He), N.V.H. (Ngo Van Hien) and N.-T.B.; supervision, N.V.H. (Ngo Van Hien); project administration, N.V.H. (Ngo Van He). All authors have read and agreed to the published version of the manuscript.

Funding: This research is funded by the Vietnam National Foundation for Science and Technology Development (NAFOSTED) under the grant number 107.03-2019.302. The authors would like to warmly express their thanks for the support.

Acknowledgments: We would be grateful for the cooperation between the Hanoi University of Science and Technology (HUST) and Shibaura Institute of Technology (SIT) in the CFD computation, guidance, and expertise. This work was also supported by the Centennial SIT Action for the 100th anniversary of Shibaura Institute of Technology to enter the top ten Asian Institutes of Technology.

Conflicts of Interest: The authors declare no conflict of interest.

References

1. Ngo, V.H.; Ikeda, Y. A Study on Application of a Commercial CFD Code to Reduce Resistance Acting on a NBT-Part 1. In Proceedings of the Japan Society of Naval Architects and Ocean Engineerings (JASNAOE), Kobe, Japan; 2012; pp. 415–418.
2. Ngo, V.H.; Ikeda, Y. Added resistance acting on hull of a non ballast water ship. *J. Mar. Sci. Appl.* **2014**, *13*, 11–12.
3. Ngo, V.H.; Ikeda, Y. Optimization of bow shape for Non Ballast Water ship. *J. Mar. Sci. Appl.* **2013**, *12*, 251–260.
4. Ngo, V.H.; Ikeda, Y. A Study on Application of CFD Code to Reduce Resistance Acting on a Non Ballast Tanker-Part 2. In Proceedings of the 6th Asia-pacific Workshop on Marine Hydrodynamics (APHydro 2012), Johor, Malaysia, 3–4 September 2012; pp. 264–269.
5. Mizutani, K.; Aoyama, S.I.Y.; Ikeda, Y.; Ngo, V.H. A Role of Spray on the added resistance acting on a blunt bow ship in head waves. In Proceedings of the 25th International Ocean and Polar Engineering Conference, Kona, Big Island, HI, USA, 21–26 June 2015; pp. 1025–1030.
6. Ikeda, Y.; Aoyama, S.I.Y.; Ngo, V.H. Development of an Appendage to Reduce the Added Resistance in Waves for Large Blunt Ship Using CFD. In Proceedings of the JASNAOE, Sendai, Japan; 2013; pp. 315–318.
7. Wnęk, A.; Soares, C.G. CFD assessment of the wind loads on an LNG carrier and floating platform models. *Ocean Eng.* **2015**, *97*, 30–36. [[CrossRef](#)]
8. Ngo, V.H.; Ikeda, K.M.Y. Effects of side guards on aerodynamic performances of the wood chip carrier. *Ocean Eng.* **2019**, *187*, 106217.
9. Ngo, V.H.; Ikeda, K.M.Y. Reducing air resistance acting on a ship by using interaction effects between the hull and accommodation. *Ocean Eng.* **2016**, *111*, 414–423.
10. Nguyen Van Trieu, N.V.H.; Ikeda, S.I.Y. Effects of turbulence models on the CFD results of ship resistance and wake. In Proceedings of the JASNAOE, Hiroshima, Japan, 27–28 November 2017; Volume 25, pp. 199–204.
11. Su, G.; Shen, H.; Su, Y. Numerical Prediction of Hydrodynamic Performance of Planing Trimaran with a Wave-Piercing Bow. *J. Mar. Sci. Eng.* **2020**, *8*, 897. [[CrossRef](#)]

12. Casalone, P.; Dell'Edera, O.; Fenu, B.; Giorgi, G.; Sirigu, S.A.; Mattiazzo, G. Unsteady RANS CFD Simulations of Sailboat's Hull and Comparison with Full-Scale Test. *J. Mar. Sci. Eng.* **2020**, *8*, 394. [[CrossRef](#)]
13. Feng, D.; Ye, B.; Zhang, Z.; Wang, X. Numerical Simulation of the Ship Resistance of KCS in Different Water Depths for Model-Scale and Full-Scale. *J. Mar. Sci. Eng.* **2020**, *8*, 745. [[CrossRef](#)]
14. Kahramanoğlu, E.; Çakıcı, F.; Doğrul, A. Numerical Prediction of the Vertical Responses of Planing Hulls in Regular Head Waves. *J. Mar. Sci. Eng.* **2020**, *8*, 455. [[CrossRef](#)]
15. Sun, H.; Zou, J.; Sun, Z.; Lu, S. Numerical Investigations on the Resistance and Longitudinal Motion Stability of a High-Speed Planing Trimaran. *J. Mar. Sci. Eng.* **2020**, *8*, 830. [[CrossRef](#)]
16. Wang, J.; Zhuang, J.; Su, Y.; Bi, X. Inhibition and Hydrodynamic Analysis of Twin Side-Hulls on the Porpoising Instability of Planing Boats. *J. Mar. Sci. Eng.* **2021**, *9*, 50. [[CrossRef](#)]
17. Tatsumi, T.; Ikeda, Y.N.Y. Development of a New Energy Saving Tanker with Non Ballast water and Podded Propulsor. In Proceedings of the 5th APHydro 2010, Osaka, Japan, 1–4 July 2010; pp. 25–28.
18. Tatsumi, T.; Ikeda, Y.N.Y. Development of a New Energy Saving Tanker with Non Ballast water-Part 1. In Proceedings of the JASNAOE, Fukuoka, Japan; 2011; pp. 216–218. (In Japanese).
19. Tatsumi, T.; Ikeda, Y.N.Y. Development of a New Energy Saving Tanker with Non Ballast water Part 2. In Proceedings of the JASNAOE, Fukuoka, Japan; 2011; pp. 219–222. (In Japanese).
20. He, N.V.; Ikeda, Y. A Study on Application of a Commercial CFD Code to Reduce Resistance Acting on a Non Ballast Tanker (Part 3) Proposed a series bow forms for non-ballast water ships. In Proceedings of the JASNAOE, Tokyo, Japan; 2012; pp. 223–226.
21. Ngo Van He, Y.N.; Ikeda, Y. A study on an optimum hull form in waves for a non ballast tankers and bulkers. In Proceedings of the 5th PAAMES and AMEC, Taipei, Taiwan, 10–12 December 2012; pp. 1–8.
22. Luo, W.; Lan, L. Design optimization of the lines of the bulbous bow of a hull based on parametric modeling and computational fluid dynamics calculation. *Math. Comput. Appl.* **2017**, *22*, 4. [[CrossRef](#)]
23. Lu, Y.; Chang, X.; Hu, A.-K. A hydrodynamic optimization design methodology for a ship bulbous bow under multiple operating conditions. *Eng. Appl. Comput. Fluid Mech.* **2016**, *10*, 330–345. [[CrossRef](#)]
24. Zhang, S.-L.; Zhang, B.-J.; Tezdogan, T.; Xu, L.-P.; Lai, Y.-Y. Research on bulbous bow optimization based on the improved PSO algorithm. *China Ocean Eng.* **2017**, *31*, 487–494. [[CrossRef](#)]
25. Lee, C.-M.; Yu, J.-W.; Choi, J.-E.; Lee, I. Effect of bow hull forms on the resistance performance in calm water and waves for 66k DWT bulk carrier. *Int. J. Naval Archit. Ocean Eng.* **2019**, *11*, 723–735. [[CrossRef](#)]
26. Begovic, E.; Bertorello, C.; Pennino, S. Experimental seakeeping assessment of a warped planing hull model series. *Ocean Eng.* **2014**, *83*, 1–15. [[CrossRef](#)]
27. He, N.V. A study on development of a new concept cargo river ship with reduced resistance acting on hull in calm water. *J. Sci. Technol.* **2017**, *121*, 89–94.
28. Najafi, A.; Nowruzzi, H. On hydrodynamic analysis of stepped planing crafts. *J. Ocean Eng. Sci.* **2019**, *4*, 238–251. [[CrossRef](#)]
29. ITTC, R. Procedures and Guidelines: Practical Guidelines for Ship CFD Applications, 7.5. 2011. Available online: <https://itcc.info/media/1357/75-03-02-03.pdf> (accessed on 20 May 2021).
30. Celik, I.B.; Ghia, U.; Freitas, C. Procedure for estimation and reporting of uncertainty due to discretization in CFD applications. *J. Fluids Eng. Trans. ASME* **2008**, *130*, 7.
31. Collie, S.; Gerritsen, M.; Jackson, P. *A Review of Turbulence Modeling for Use in Sail Flow Analysis*; School of Engineering, University of Auckland: Auckland, New Zealand, 2001; Report.
32. Xia, M.; Jiang, L. Application of an unstructured grid-based water quality model to Chesapeake Bay and its adjacent coastal ocean. *J. Mar. Sci. Eng.* **2016**, *4*, 52. [[CrossRef](#)]
33. Windt, C.; Davidson, J.; Schmitt, P.; Ringwood, J.V. On the Assessment of Numerical Wave Makers in CFD Simulations. *J. Mar. Sci. Eng.* **2019**, *7*, 47. [[CrossRef](#)]
34. Procedures, R. Guidelines, Practical Guidelines for Ship CFD Application. In Proceedings of the 27th International Towing Tank Conference (ITTC), Copenhagen, Denmark, 31 August–5 September 2014.
35. He, N.V. A study on reduced air resistance acting on hull of a cargo river ship by used CFD. *J. Sci. Technol. Vietnam* **2018**, *127B*, 50–56.
36. He, N.V.; Hien, N.V.; Truong, V.-T.; Bui, N.-T. Interaction Effect between Hull and Accommodation on Wind Drag Acting on a Container Ship. *J. Mar. Sci. Eng.* **2020**, *8*, 930. [[CrossRef](#)]
37. Windt, C.; Davidson, J.; Ransley, E.J.; Greaves, D.; Jakobsen, M.; Kramer, M.; Ringwood, J.V. Validation of a CFD-based numerical wave tank model for the power production assessment of the wavestar ocean wave energy converter. *Renew. Energy* **2020**, *146*, 2499–2516. [[CrossRef](#)]
38. Schmitt, P.; Windt, C.; Davidson, J.; Ringwood, J.V.; Whittaker, T. The Efficient Application of an Impulse Source Wavemaker to CFD Simulations. *J. Mar. Sci. Eng.* **2019**, *7*, 71. [[CrossRef](#)]
39. Wheeler, M.P.; Matveev, K.I.; Xing, T. Numerical Study of Hydrodynamics of Heavily Loaded Hard-Chine Hulls in Calm Water. *J. Mar. Sci. Eng.* **2021**, *9*, 184. [[CrossRef](#)]